THE FIRST MOMENT OF G_1 MEASURED WITH THE CLAS DETECTOR

G. E. DODGE

Department of Physics
Old Dominion University
Norfolk, VA 23529, USA
E-mail: dodge@physics.odu.edu

FOR THE CLAS COLLABORATION

A large program of spin structure function measurements is underway in Jefferson Lab's Hall B. Of particular interest is the first moment of the spin structure function g_1, which goes through a rapid transition from the photon point ($Q^2 = 0$), where it is constrained by the Gerasimov-Drell-Hearn sum rule, to the deep inelastic limit where it is sensitive to the nucleon spin fraction carried by quarks. One can then study the transition from hadronic to quark degrees of freedom over the whole range of Q^2. We use polarized electrons incident on polarized NH_3 and ND_3 targets to study proton and deuteron spin observables in and above the resonance region. Using the Cebaf Large Acceptance Spectrometer (CLAS) and beam energies of 1.6, 2.4, 4.2 and 5.7 GeV, we are able to cover a wide kinematic range: 0.05 GeV^2 $< Q^2 <$ 5.0 GeV^2 and $W <$ 3.2 GeV. We will describe the experiment and present the GDH and Bjorken integrals using the 1.6 and 5.7 GeV data.

1. Introduction

Investigation of the structure of the nucleon using polarization observables continues to be of great interest to the nuclear physics community. The inclusive electron scattering cross section can be written as

$$\frac{d\sigma}{dE'd\Omega} = \Gamma_v \left[\sigma_T + \epsilon\sigma_L + P_e P_t \left(\sqrt{1-\epsilon^2} A_1 \sigma_T \cos\Psi + \sqrt{2\epsilon(1-\epsilon)} A_2 \sigma_T \sin\Psi\right)\right] \quad (1)$$

where σ_T and σ_L are the longitudinal and transverse cross sections, Ψ is the angle between the target polarization and the three-momentum transfer q, and P_e and P_t are the electron beam and target polarization, respectively. Γ_v is the virtual photon flux and ϵ is the polarization of the virtual photon.

The transverse photon asymmetry

$$A_1(\nu, Q^2) = \frac{\sigma^{\frac{1}{2}} - \sigma^{\frac{3}{2}}}{\sigma^{\frac{1}{2}} + \sigma^{\frac{3}{2}}} \stackrel{\lim Q^2 \to \infty}{\longrightarrow} \frac{\Sigma e_i^2 \Delta q_i(x)}{\Sigma e_i^2 q_i(x)} = \frac{g_1(x)}{F_1(x)} \tag{2}$$

is sensitive to the quark structure of the nucleon. Here the absorption cross section for real or virtual transverse photons incident upon the nucleon is given by $\sigma^{\frac{1}{2}}$ and $\sigma^{\frac{3}{2}}$ for total helicity $\frac{1}{2}$ and $\frac{3}{2}$, respectively. $\Delta q_i/q_i$ is the net polarization of quarks of flavor i in the direction of the nucleon spin and q_i is the probability of finding a quark of flavor i in the nucleon. The unpolarized structure functions F_1 and F_2 and the spin structure functions g_1 and g_2 are functions of the four-momentum transfer squared Q^2 and the quark momentum fraction $x = \frac{Q^2}{2M\nu}$, where ν is the energy of the virtual photon. $A_2 = \frac{\sigma_{LT}}{\sigma_T}$, where σ_{LT} is the longitudinal-transverse interference cross section.

There is particular interest in the first moment of g_1, $\Gamma_1(Q^2) = \int_0^{1-} g_1(x, Q^2)dx$, which is constrained at low Q^2 by the Gerasimov-Drell-Hearn sum rule[1] and at high Q^2 by the Bjorken sum rule[2] and previous deep inelastic scattering (DIS) experiments. In our definition the upper limit of the integral does not include the elastic peak. Ji and Osborne[3] have shown that the GDH sum rule can be generalized to all Q^2 via

$$S_1(\nu = 0, Q^2) = \frac{8}{Q^2} \left[\Gamma_1(Q^2) + \Gamma_1^{el}(Q^2)\right], \tag{3}$$

where $S_1(\nu, Q^2)$ is the spin-dependent virtual photon Compton amplitude. S_1 can be calculated in Chiral Perturbation Theory (χPT) at low Q^2 and with perturbative QCD (pQCD) at high Q^2. There is some hope that lattice QCD will one day be able to fill in the intermediate Q^2 range. In Γ_1 we have a calculable observable that spans the entire energy range from hadronic to partonic descriptions of the nucleon. Furthermore, one can use Γ_1 and the Bjorken integral $\Gamma_1^p - \Gamma_1^n$ to extract higher twist parameters[4] which are sensitive to quark-gluon and quark-quark correlations in the nucleon at moderate Q^2.

At Jefferson Lab there is a comprehensive program of spin structure measurements underway in all three experimental halls. These experiments typically use longitudinally polarized electrons incident on longitudinally or transversely polarized targets to measure the spin structure functions g_1 and g_2. Here we report on measurements in Hall B, collectively known as "EG1."

2. EG1 Experiment

In the EG1 experiment we scatter longitudinally polarized electrons from longitudinally polarized proton (NH_3) and deuterium (ND_3) targets. The beam was produced from a strained GaAs wafer and had an average polarization of 70% as measured by a Moller polarimeter. The polarization of the electrons was flipped at 30 Hz pseudo-randomly, meaning that the helicity of the first of two polarization states was chosen randomly and was always followed by the opposite polarization. The beam was rastered over the face of the target cell to avoid heating and depolarization. The current varied from 0.3 nA to 10 nA depending on the beam energy, torus configuration and target.

The target[5] was polarized in a 5 T magnetic field produced by a pair of Helmholtz coils. The NH_3 and ND_3 crystals were held in a 1 K liquid helium bath. Microwaves were used to dynamically enhance the polarization of the proton or deuteron via spin transfer from unpaired electrons in the ammonia. The proton polarization ranged from 70–90% and the deuteron polarization varied from 10–35%. Data were also taken with ^{12}C, ^{4}He and frozen ^{15}N to determine the dilution from unpolarized material in the target.

Scattered electrons and other final state particles were detected in the Cebaf Large Acceptance Spectrometer (CLAS) in Hall B.[6] The heart of the CLAS is a toroidal magnetic field produced by six superconducting coils which divide the detector into six sectors. Data were taken with the field oriented in both directions, so that electrons were deflected toward the beamline (inbending configuration) and away from the beamline (outbending configuration) in order to increase the kinematic range coverage in Q^2. Each sector consists of three layers of drift chambers for measuring particle momenta, time-of-flight scintillators to aid in particle identification, a Cherenkov gas counter to separate electrons from pions and an electromagnetic calorimeter for additional suppression of electron misidentification. Data acquisition was triggered by a coincidence between the Cherenkov detector and the calorimeter in one of the six sectors. The large acceptance of the CLAS detector enables us to take data over a wide kinematic range at one time.

All data (over 25 billion triggers) for EG1 have been taken in two runs, in 1998 (EG1a) and 2000–2001 (EG1b), with beam energies of 1.6, 2.4, 4.2 and 5.7 GeV. Inclusive results from the smaller EG1a data set have been published.[7,8] The EG1b data set extends the kinematic coverage to both

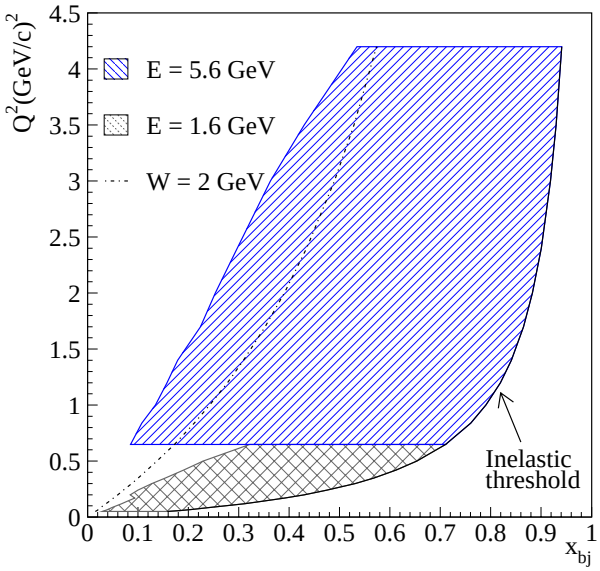

Figure 1. Kinematic coverage for EG1 for the 1.6 GeV (parallel line shaded region) and 5.7 GeV (cross-hatched shaded region) data.

lower and higher Q^2 and higher W, and has significantly better statistical accuracy. Here we report on the analysis of the 1.6 and 5.7 GeV EG1b data. Figure 1 shows the range in Q^2 and x ($W \leq 3.2$ GeV) covered by our combined 1.6 and 5.7 GeV data sets. Our data include multi-particle final states, making it possible to investigate exclusive[9] and semi-inclusive[10] pion production, deeply virtual Compton scattering[11] and other exclusive channels.[9]

3. Data Analysis

The raw asymmetries are corrected for the beam charge asymmetry, the dilution factor and radiative effects. Since the elastic peak is in our acceptance, the product of beam and target polarization is determined from the known ep elastic asymmetry. Our target is polarized along the beam direction, rather than along the virtual photon helicity, so we extract a combination of A_1 and A_2:

$$A_1 + \eta A_2 = \frac{1}{D P_e P_t} A_{raw}, \tag{4}$$

where the depolarization factor $D = \frac{1-E'\epsilon/E}{1+\epsilon R}$, E (E') is the beam (scattered electron) energy, $R \lesssim 0.2$ is the ratio of the longitudinal to the transverse photoabsorption cross section and $\eta = \frac{\epsilon\sqrt{Q^2}}{E-E'\epsilon}$. Finally, using a parameterization[12] of the world data to model F_1, A_2 and R, we extract g_1

$$g_1(x,Q^2) = \frac{F_1}{1+\gamma^2}(A_1 + \gamma A_2), \tag{5}$$

where $\gamma^2 = \frac{Q^2}{\nu^2}$. Our parameterization includes input from phenomenological models AO[13] and MAID[14] as well as the EG1a data in the resonance region.

4. Results

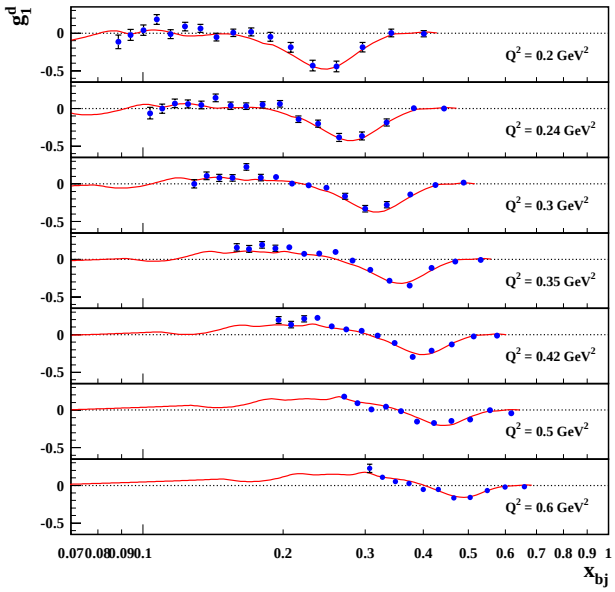

Figure 2. Preliminary results for $g_1^d(x,Q^2)$ for the 1.6 GeV (inbending) data. A model parameterizing all world data is shown as the solid line.[12]

Preliminary results for the spin structure function $g_1^d(x,Q^2)$ at 1.6 and 5.7 GeV are shown in Figures 2 and 3. Similar figures for $g_1^p(x,Q^2)$ can

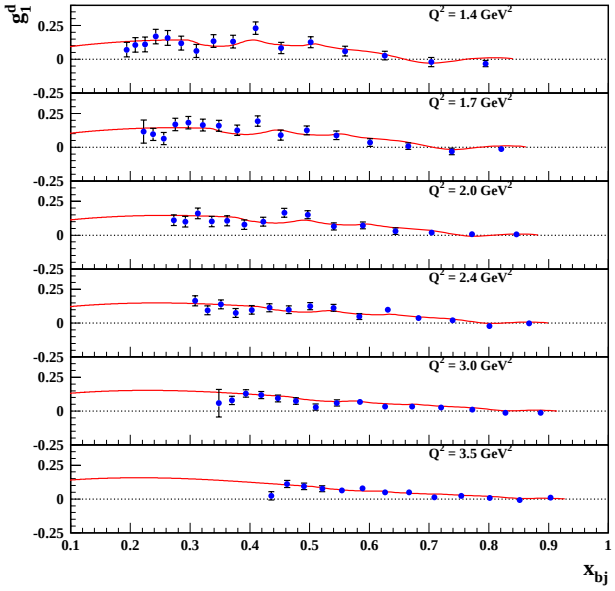

Figure 3. Same as Fig. 2 except for the 5.7 GeV (inbending and outbending) data.

be found elsewhere.[17] At low momentum transfers the negative $\Delta(1232)$ resonance is quite prominent but it decreases steadily in strength as Q^2 increases. The higher mass resonances make a rapid transition from nearly zero to rather large positive values of g_1. The first moment of g_1^d is shown in Figure 4. We see the integral turn over at low Q^2, consistent with the slope predicted by the GDH sum rule. In general the data are well described by a phenomenological model[13] which includes all resonances and a VMD-inspired transition to the DIS limit. After the 2.4 and 4.2 GeV data are analyzed, the intermediate Q^2 region will be covered with good precision.

Γ_1 at low Q^2 is especially interesting because χPT calculations should be valid there. The low Q^2 Γ_1^d data are shown in more detail in Figure 5. Here one can see that the calculation of Ji *et al.*[19] is consistent with the data up to roughly $Q^2 = 0.1$ GeV^2. Figure 5 shows the central value of the χPT calculation by Bernard *et al.*[18], but does not show the range of uncertainty in that prediction, which includes the data. Ongoing work to reduce that uncertainty has been reported at this meeting.[20] Data have been taken in Hall A[21] and an experiment is planned for Hall B[22] to provide additional precise measurements in the low Q^2 region.

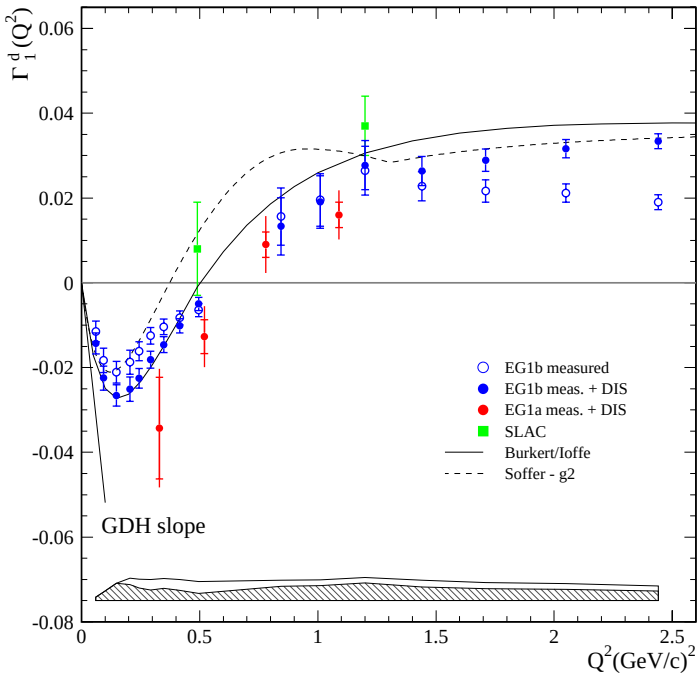

Figure 4. Preliminary results for Γ_1^d. The EG1a[7] and SLAC[15] data are shown as the solid red circles and green squares, respectively. The open blue circles represent the integral of the EG1b data over the measured kinematic region and the closed blue circles include an extrapolation over the unmeasured part of the x spectrum using a model of world data. Phenomenological models by Burkert and Ioffe[13] and Soffer and Teryaev[16] are represented by solid and dashed lines, respectively. The dark shaded band indicates the experimental systematical error, while the additional area includes the extrapolation uncertainties.

Figure 6 shows the Bjorken integral, $\Gamma_1^p - \Gamma_1^n$, as a function of Q^2, where the EG1b proton and deuteron data have been combined to extract information on the neutron (closed circles). For comparison, the results from EG1a are shown as the open squares. Combining Hall A neutron results with the (larger uncertainty) EG1a proton data results in the closed triangles. The data are consistent with the model by Burkert and Ioffe and with the leading twist pQCD calculation. One expects the range of validity for χPT calculations to be extended, since contributions from the Delta resonance should cancel in the proton-neutron difference. The calculation by Ji *et al.* follows that expectation and is consistent with the data up to roughly $Q^2 = 0.25$ GeV^2. Again the uncertainty band for the calculation

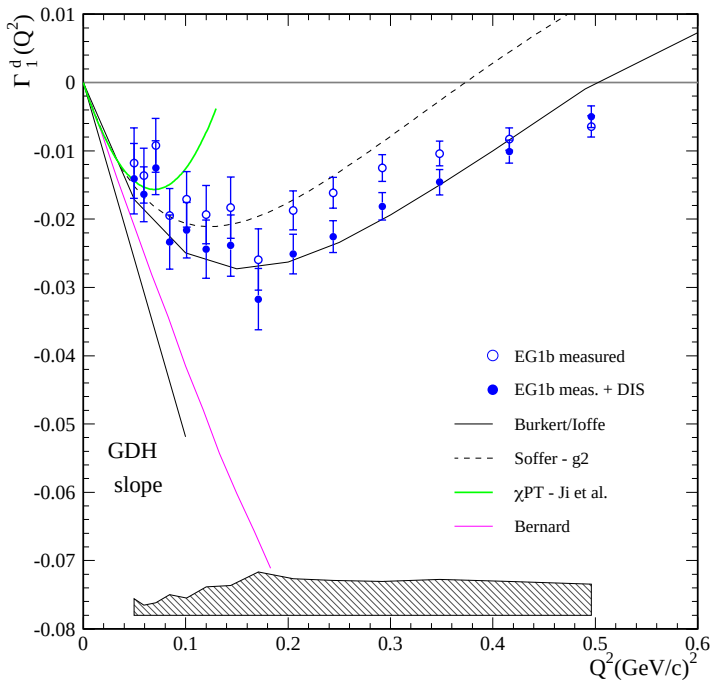

Figure 5. Preliminary results for Γ_1^d at low Q^2. χPT calculations from Bernard[18] and Ji[19] are shown as the heavy and light dotted lines, respectively. Phenomenological models by Burkert and Ioffe[13] and Soffer and Teryaev[16] are represented by solid and dashed black lines, respectively.

by Bernard *et al.* includes the data.

5. Outlook

In this talk we have reported only on the EG1 results for g_1 and its first moment, including the Bjorken integral. There are many other interesting topics that can be addressed with these data, including the behavior of A_1 at large x,[17,24] $\Delta u/u$ and $\Delta d/d$ and higher twist effects.[4] There is also the question of the range of validity of local quark-hadron duality, which has been demonstrated in unpolarized structure functions.[25] One can look for similar behavior in polarized structure functions with our high quality measurements of g_1 over a wide range in x and Q^2 in and above the resonance region.[24]

Next we will analyze the 2.4 and 4.2 GeV data, which will enable us to

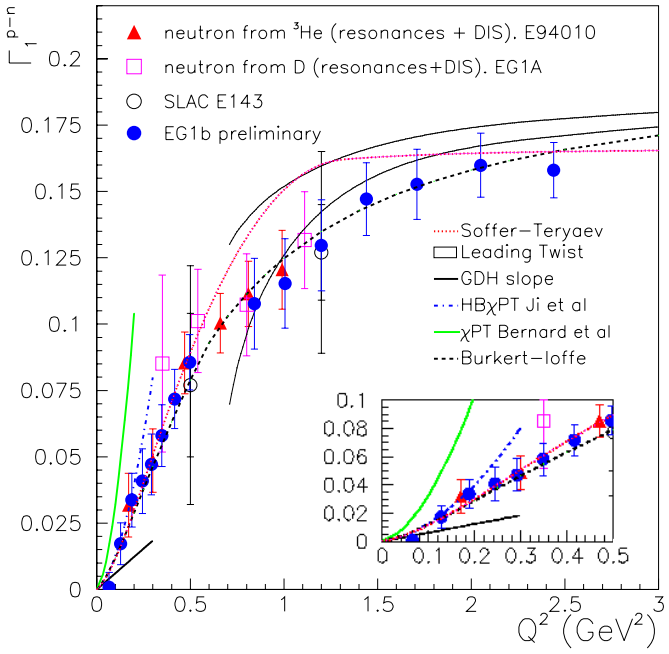

Figure 6. Preliminary results for $\Gamma_1^p - \Gamma_1^n$. The closed circles represent the preliminary EG1b data in which the neutron was extracted from the deuteron and the proton. The open squares represent the same calculation using the EG1a data[8,7] (proton and deuteron). The closed triangles were determined using the Hall A neutron results[23] and the EG1a proton results.[8] SLAC data[15] are shown as the open circles. χPT calculations by Bernard[18] and Ji[19] are shown as the solid and dash-dot curves, respectively. Phenomenological models by Burkert and Ioffe[13] and Soffer and Teryaev[16] are represented by dashed and dotted lines, respectively.

improve the statistical precision of our results for g_1 and Γ_1 at intermediate Q^2 as well as extend our coverage in W at low and moderate Q^2, thus reducing our systematic error. It is precisely in the intermediate Q^2 region that higher precision data are needed on the Bjorken integral in order to extract higher twist parameters and to pin down the onset of duality in g_1. Finally, we will extract information about the spin structure of the neutron, by working closely with theorists to understand nuclear and binding effects.

Together with results from Halls A[23] and C[26] these new data should lead to an improved understanding of the spin structure of the nucleon in the transition to the scaling regime.

Acknowledgments

This research is supported by the US Department of Energy under grant DE-FG02-96ER40960.

References

1. S. Gerasimov, *Sov. J. Nucl. Phys.* **2**, 430 (1966); S.D. Drell and A.C. Hearn, *Phys. Rev. Lett.* **16**, 908 (1966).
2. J.D. Bjorken *et al.*, *Phys. Rev.* **148**, 1467 (1966).
3. X. Ji and J. Osborne, *J. Phys. G: Nucl. Part. Phys.* **27**, 127 (2001).
4. A. Deur, these proceedings.
5. C.D. Keith *et al.*, *Nucl. Inst. and Meth. Phys. Res., Sect. A* **501**, 327 (2003).
6. B.A. Mecking *et al.*, *NIMA* **503**, 513 (2003).
7. J. Yun *et al.*, *Phys. Rev. C* **67**, 055204 (2003).
8. R. Fatemi *et al.*, *Phys. Rev. Lett.* **91**, 222002 (2003).
9. A. Biselli, these proceedings.
10. H. Avakian, these proceedings.
11. S. Chen *et al.*, these proceedings.
12. S.E. Kuhn, private communication.
13. V.D. Burkert and B.L. Ioffe, *Phys. Lett. B* **296**, 223 (1992); V.D. Burkert and B.L. Ioffe, *J. Exp. Theor. Phys.* **78**, 619 (1994).
14. D. Drechsel and L. Tiator, *J. Phys. G: Nucl. Part. Phys.* **18**, 449 (1992).
15. K. Abe *et al.*, *Phys. Rev. Lett.* **78**, 815 (1997).
16. J. Soffer and O.V. Teryaev, *Phys. Rev. D* **51**, 25 (1995); J. Soffer and O.V. Teryaev, *Phys. Lett. B* **545**, 323 (2002).
17. Y. Prok, these proceedings.
18. V. Bernard *et al.*, *Phys. Rev. D* **67**, 076008 (2003).
19. X. Ji *et al.*, *Phys. Lett. B* **472**, 1 (2000).
20. Ulf-G. Meissner, these proceedings.
21. J.-P. Chen, A. Deur, F. Garibaldi, "The GDH Sum Rule and the Spin Structure of ^{3}He and the Neutron Using Nearly Real Photons," Jefferson Lab E97-110 (1997).
22. M. Battaglieri, A. Deur, R. De Vita, M. Ripani, "The GDH Sum Rule with Nearly-Real Photons and the Proton g_1 Structure Function at Low Momentum Transfer," Jefferson Lab proposal E03-006 (2003).
23. M. Amarian *et al.*, *Phys. Rev. Lett.* **89**, 242301 (2002); M. Amarian *et al.*, *Phys. Rev. Lett.* **92**, 022301 (2004); X. Zheng *et al.*, *Phys. Rev. Lett.* **92**, 012004 (2004).
24. T.A. Forest, these proceedings.
25. I. Niculescu *et al.*, *Phys. Rev. Lett.* **85**, 1182 (2000); I. Niculescu *et al.*, *Phys. Rev. Lett.* **85**, 1186 (2000).
26. O.A. Rondon, "TJNAF Exp. 96-002/01-006: Precision measurement of the nucleon spin structure functions in the region of the nucleon resonances," Jefferson Lab E01-006 (2001); C. Keppel, "Measurement of $R = \sigma_L/\sigma_T$ in the Nucleon Resonance Region," Jefferson Lab E94-110 (1994).